SCIENTIFIC REPORTS

OPEN

SUBJECT AREAS:
CONFOCAL MICROSCOPY
CELLULAR IMAGING

Received
17 June 2014

Accepted
19 November 2014

Published
10 February 2015

Correspondence and requests for materials should be addressed to Y.L. (yizhi_liu@aliyun.com)

* These authors contributed equally to this work.

Quantitative analysis of injury-induced anterior subcapsular cataract in the mouse: a model of lens epithelial cells proliferation and epithelial-mesenchymal transition

Wei Xiao*, Xiaoyun Chen*, Weihua Li, Shaobi Ye, Wencong Wang, Lixia Luo & Yizhi Liu

State Key Laboratory of Ophthalmology, Zhongshan Ophthalmic Center, Sun Yat-sen University, Guangzhou, People's Republic of China.

The mouse lens capsular injury model has been widely used in investigating the mechanisms of anterior subcapsular cataract (ASC) and posterior capsule opacification (PCO), and evaluating the efficacy of antifibrotic compounds. Nevertheless, there is no available protocol to quantitatively assess the treatment outcomes. Our aim is to describe a new method that can successfully quantify the wound and epithelial-mesenchymal transition (EMT) markers expression *in vivo*. In this model, lens anterior capsule was punctured with a hypodermic needle, which triggered lens epithelial cells (LECs) proliferation and EMT rapidly. Immunofluorescent staining of injured lens anterior capsule whole-mounts revealed the formation of ASC and high expression of EMT markers in the subcapsular plaques. A series of sectional images of lens capsule were acquired from laser scanning confocal microscopy (LSCM) three-dimensional (3D) scanning. Using LSCM Image Browser software, we can not only obtain high resolution stereo images to present the spatial structures of ASC, but also quantify the subcapsular plaques and EMT markers distribution sucessfully. Moreover, we also demonstrated that histone deacetylases (HDACs) inhibitor TSA significantly prevented injury-induced ASC using this method. Therefore, the present research provides a useful tool to study ASC and PCO biology as well as the efficacy of new therapies.

Cataract is the most common cause of visual deterioration in the elderly all over the world[1]. Anterior subcapsular cataract (ASC) and posterior capsule opacification (PCO) are two different types of cataract, but they share similar molecular and cellular mechanisms[2,3]. PCO, also known as a secondary cataract, is the most common long-term complication of cataract surgery[4]. In the past few decades, plentiful studies tried to find various kinds of interventions to inhibit PCO, including modifications of surgical techniques and intraocular lens designs, implantation of additional devices and pharmacological treatment[4]. However, the incidence of PCO is still approximately 20% to 40% in adults and 100% in children[5,6]. So far, cataract surgery and Nd:YAG laser capsulotomy are the only effective therapies for ASC and PCO, meanwhile, they are likely to induce many other complications and risks. Therefore, a better understanding of ASC and PCO pathogenesis is critical for the development of new pharmacologic treatments.

Nowadays, histological evidence shows that proliferation and epithelial-mesenchymal transition (EMT) of lens epithelial cells (LECs) are the crucial pathological mechanisms in the development of ASC[7,8] and PCO[9,10]. ASC is a primary cataract which is mainly caused by ocular trauma, inflammation or irritation[11], while PCO is caused by a wound healing response of residual LECs after cataract surgery. After trauma, irritation or surgery, various cytokines and growth factors levels increase in the aqueous humor and stimulate LECs to proliferate and undergo EMT[4]. Transforming growth factor β (TGFβ), especially TGFβ2, the major isoform in the aqueous humour, plays a vital role in the cell biology of ASC and PCO[12]. During the process of EMT, LECs undergo cytoskeletal rearrangment, transform from epithelial phenotype to mesenchymal phenotype, with the addition of a large amount of extracellular matrix proteins (ECM) deposition, such as collagen and fibronectin. For ASC, the proliferation and EMT of LECs *in situ* lead to the formation of subcapsular plaque just beneath the lens anterior

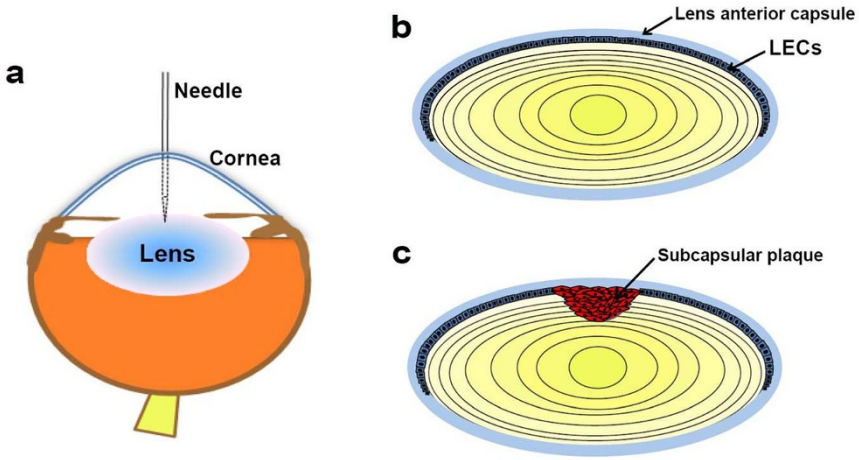

Figure 1 | Cartoon schematic of the mouse lens anterior capsule injury model. (a) The anterior capsule of mouse lens is punctured with a hypodermic needle through the cornea, which initiates wound repair response rapidly and reach maximum after 7 days. (b) Schematic diagram of the normal lens shows the lens epithelium is a typical single cuboidal epithelium which sits on lens capsule. (c) After injury, LECs may proliferate, undergo EMT, and migrate from the epithelial sheet, finally become multicellular mass and subcapsular plaque in the injured region of the lens.

capsule[13]. However, in the development of PCO, the residual LECs migrate away from the original location onto the posterior capsule, contributing to the formation of plaque beneath the posterior capsule[4,8].Thus, inhibition of LECs proliferation and EMT may be a promising strategy to prevent ASC and PCO.

In order to have a better understanding of the development of ASC, mouse lens capsular injury model has been established to study the molecular and cellular mechanisms *in vivo* that underpin ASC formation. Emergence of this animal model, therefore, not only enables us to have a more comprehensive understanding of the etiology of ASC at a molecular level, but also fulfills the need for drug screening tool. Moreover, the availability of transgenic and knockout mice allows researchers to investigate the role of particular genes in the development of ASC. In this model, the anterior capsule of mouse lens is punctured with a hypodermic needle that initiates wound repair response rapidly. During this process, TGFβ/Smad pathway is activated between 4–8 h after anterior capsular injury and lasts about 3 d[14]. Afterwards, TGFβ induces the accumulation of ECM components (collagens I and IV) around the cells in injured mouse lenses in a later phase of repair[14]. Accumulation of ECM molecules in the region of wound repair might also be a factor in stimulating proliferation, since these molecules are known to promote proliferation of LECs in vitro[15]. LECs may proliferate, undergo EMT, increase motility and invasion, and migrate from the epithelial sheet, finally become multicellular mass and subcapsular plaque in the injured region of the lens[16]. To date, paraffin section of injured lenses and histological staining are widely used to monitor the subcapsular plaques development by microscopic examination. However, traditional two-dimensional histological image cannot provide spatial information and thick samples photographed with bright field microscopy are liable to lose their definition. Routine paraffin section and histological staining cannot identify multiple antigens in different cells, as well as co-localized antigens in the same cell. In addition, fixing solution and embedding materials can result in the loss of tissue antigenicity, making it difficult to perform immunochemical and immunofluorescent staining on the sections. What's more, quantification of the anterior subcapsular plaque using paraffin section and histological staining is a technically immense challenge, tedious, and time-consuming procedure. It requires considerable section skills and is susceptible to distortion and sample losses. Firstly, the injured region of the lens is needed to be sectioned serially and collected all the sections successfully which contain the beginning and the end of the subcapsular plaque. Secondly, to calculate the volume of the subcapsular plaque, all the paraffin sections are needed to be stained and obtained all microscopic images. Hence, a better quantitative method is critical for the evaluation of the injured region of the lens and drug therapeutic effect.

In this study, we employed a simple, good reproducibility and effective lens anterior capsule whole-mount immunofluorescent staining method that allows us to successfully and efficiently quantify the volumes of the subcapsular plaques in mouse lens capsular injury model using laser scanning confocal microscopy (LSCM) three-dimensional (3D) imaging. In addition, this method enables us to observe the spatial features of the subcapsular plaques in detail from any viewing direction and position. Combined with various markers specific for EMT and ECM compoments, it can also allow us to quantitatively analyze EMT markers distribution and ECM components deposition in this model.

Results

An EMT model of ASC. According to current knowledge, the lens epithelium is a typical single cuboidal epithelium which sits on lens capsule[17]. The central anterior epithelial region is considered to be quiescent, whereas cells in the peripheral germinative regions are mitotically active[17]. Mechanical wounding of the central epithelium is able to recruit the cells in the peripheral germinative regions to proliferate in injury and repair of the epithelium[18]. Therefore, mouse lens capsular injury model has been established to study the molecular and cellular mechanisms *in vivo* that underpin ASC formation. As illustrated in Fig. 1, the central lens anterior capsule of the mouse eye was punctured with a 26-gauge hypodermic needle through the central cornea, which initiates wound repair response rapidly[14,19]. During this process, LECs may proliferate, undergo EMT, increase motility and migrate from the epithelial sheet, finally become multicellular mass and subcapsular plaque in the injured region of the lens (Fig. 1). This model is easily performed and the results are highly reproducible.

Fluorescence microscope analyses of injured lens anterior capsules. To observe the central and the peripheral sites of the injury of lens anterior capsules, the lens anterior capsule whole-mounts were examined for the first time using fluoresence microscope with low and high magnification. As shown in Fig. 2, immunofluorescent staining of lens anterior capsules after injury for 7 days revealed distinct evidence of ASC formation including extensive multilayer of cells forming plaques beneath the anterior lens capsules. By contrast, the lens epithelium in the peripheral sites of the injury remained single layer epithelium. The expression of α-

SMA and vimentin, the hallmarks of the myofibroblasts, and Col I which is a major component of the pathological ECM, were examined in injury-induced ASC formation. Expression of α-SMA increased dramatically in the subcapsular plaques of the injured lens, whereas lens epithelium in the normal lens and the peripheral site of the injury had no α-SMA expression. In the normal lens epithelium, vimentin expression is relatively low and collagen expression is confined to the lens capsule, however, high expression of vimentin and aberrant Col I deposition were observed in the subcapsular plaques of the injured lens. These histological findings suggestd mechanical wounding of the central lens epithelium can stimulate cells to proliferate, undergo EMT, migrate to the injury, and repair the epithelium. Immunofluorescent staining of lens anterior capsule whole-mount is a effective method to observe the subcapsular plaques of the injured lens.

Confocal microscope 2D analyses of EMT markers kinetic expression in the injured lens anterior capsules. To further explicitly observe microstructures of the subcapsular plaques and kinetically monitor EMT markers expression in the injured region of lens anterior capsule, a LSCM with higher resolution was used. 2D confocal images showed that when the lenses were injuried for 3 days, a large number of LECs proliferated, migrated from the epithelial sheet and gathered around the capsular break, as well as EMT markers α-SMA, Col I and vimentin were aready detected in the capsule injured region (Fig. 3a). At day 5 after injury, more and more LECs assembled and developed multilayer LECs mass beneath the lens anterior capsule, moreover, increased EMT markers expression were obsered. At day 7 after injury, distinct subcapsular plaques in the injured region of the lenses were observed and the expression of EMT markers were markedly increased (Fig. 3a). However, the closer to the central of the injury, the stronger staining of α-SMA, Col I and vimentin were detected. Epithelial cells distal to the injury site were not labeled at these. Due to lens anterior capsule whole-mount cannot provide vertical section information of the wound, so we combined it with immunofluorescent staining of cryosection to examine the vertical section of lens capsular wound. Cryosection staining also revealed that the subcapsular plaque is composed of aberrant fibroblast-like cells and abundant ECM deposition, and the morphology of the subcapsular plaque is similar to trustum of a pyramid (Fig. 3b). These results indicated that LSCM imaging can provide us with more explicite 2D images compared with routine fluorescent microscope.

Confocal microscope 3D analyses of injured lens anterior capsules. To reveal 3D architectures of the subcapsular plaques of the injured lens, a series of the lens anterior capsule whole-mount images were reconstructed using LSCM Image Browser software for stereo projection. Figure 4 are stereo projections of confocal serial images that exhibit representative 3D subcapsular plaques at day 7. A 360-degree rotation view of the subcapsular plaques can be automatically played by using ANIM tool or manually viewed at any direction by dragging SLICE tool. Fig. 4a is lens capsule projections of the holistic views of the subcapsular plaques, which shows the maximal areas of the subcapsular plaques. Fig. 4b presents the lens capsules from 90-degree rotation projection angle, which marks the depth where the base of the subcapsular plaques could reach. These images suggested that LSCM 3D scanning provides an entirely new approach to present the spatial structures of the subcapsular plaques with high resolution.

Quantification the sizes of the subcapsular plaques. To observe morphology of the subcapsular plaques and the distribution of EMT markers in detail from different depth, continuous images of Z-series from the buttom to the top of the subcapsular plaque at day 7 were revealed in Fig. 5. Furthermore, in order to quantify the sizes of the subcapsular plaques and EMT markers distribution *in situ*, the LSCM Image Browser software was used. As described in Fig. 6a and b, the areas of the subcapsular plaque and EMT marker distribution in each image can be measured through defining the target objects with DRAWING tool and quantified with MEASURE tool. Afterwards, the volumes of the subcapsular plaque and EMT marker distribution in every two images were calculated according to the formula of the volume of pyramid, and the total volumes of them equal to the sum total of every two images. Using this method, quantification analyses showed that the volumes of the subcapsular plaques and EMT markers distribution were progressively increased

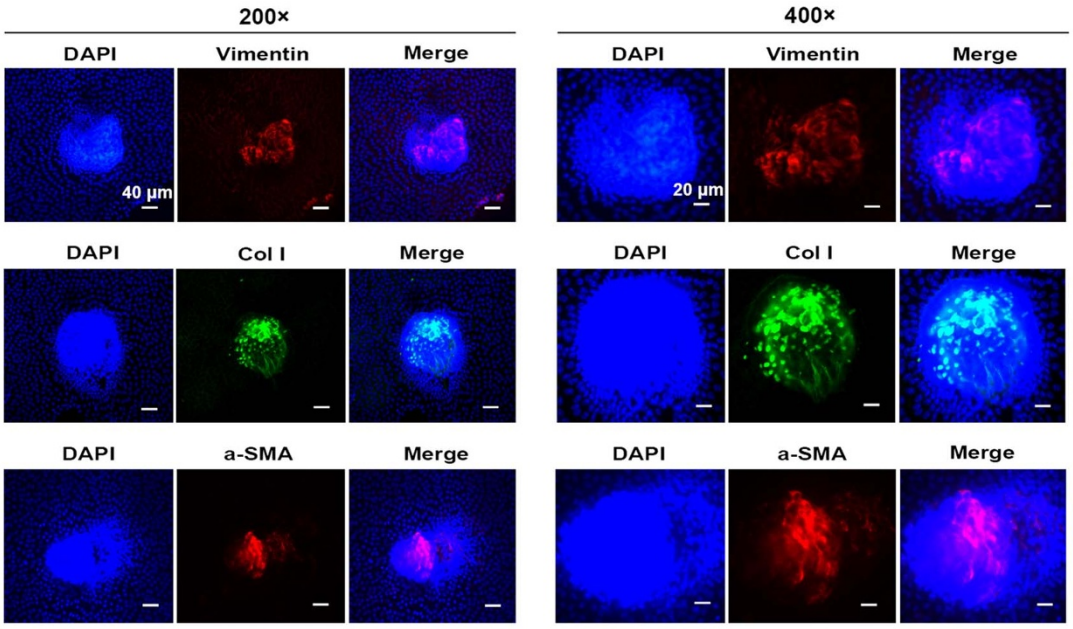

Figure 2 | Fluorescence microscope analyses of injured lens anterior capsules. Lens anterior capsules were isolated after injury for 7 days and used for whole-mount staining with LECs nuclei (blue) and EMT markers vimentin (red), Col I (green), and α-SMA (red). Images were acquired from fluorescence microscope with low (200×) and high magnification (400×). Scale bar = 40 and 20 μm, respectively.

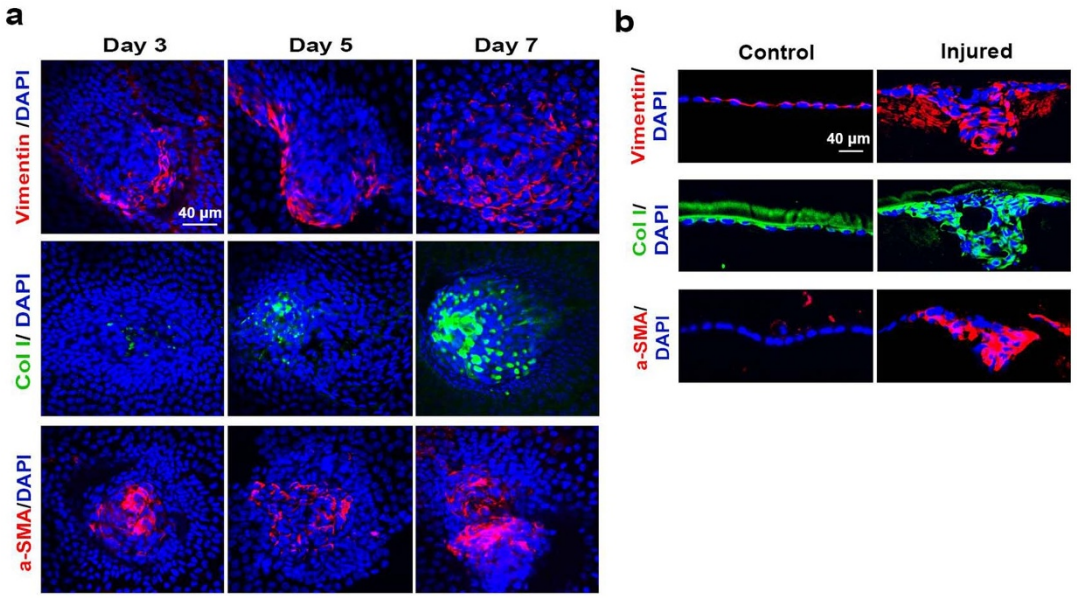

Figure 3 | Confocal microscope 2D analyses of EMT markers kinetic expression in the injured lens anterior capsules. (a) Lens anterior capsules were isolated after injury for 3, 5 and 7 days and used for whole-mount staining with LECs nuclei (blue) and EMT markers vimentin (red), Col I (green), and α-SMA (red). Images were obtained from LSCM 2D scanning. Scale bar = 40 μm. (b) Cryosections of injured lens at day 7 were stained with EMT markers vimentin (red), Col I (green), and α-SMA (red), and images were obtained from LSCM 2D scanning. Scale bar = 40 μm.

after injury (Fig. 6c). Because there are no physical sections involved in sample preparation, the errors from distotions and artifacts can be minimized. These data indicated that LSCM 3D imaging gives us a chance to quantify the volumes of the subcapsular plaques and EMT hallmarks distribution in mouse lens capsular injury model efficiently and sucessfully.

Histone deacetylases (HDACs) inhibitor TSA suppressed injury-induced ASC in the mouse lens capsular injury model. Multiple studies have suggested that histone deacetylases (HDACs)-mediated epigenetic mechanism plays a central role in the pathogenesis of various diseases, including cancers, inflammatory diseases, metabolic disorders and fibrotic diseases[20–22]. For this reason, HDAC inhibitors now are promising new compounds for the therapy of cancers[23,24] and fibrotic diseases[21,25]. Our previous study also demonstrated that HDAC inhibitor TSA strongly suppressed TGFβ2-induced EMT of LECs *in vitro* and ASC in the whole lens culture semi-*in vivo* model[13]. To prove lens capsule whole-mount combined with LSCM 3D imaging this quantitative method can be used to evaluate the efficacy of new therapies, the effect of TSA in

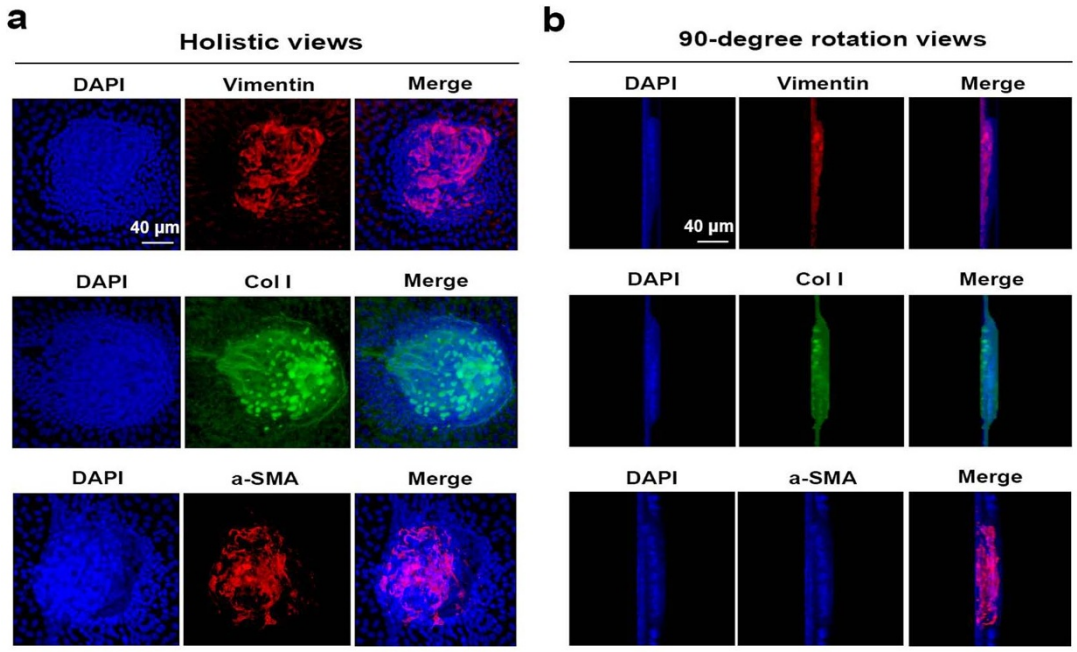

Figure 4 | Confocal microscope 3D analyses of injured lens anterior capsules. The injured lens anterior capsules at day 7 were used for whole-mount staining with LECs nuclei (blue) and EMT markers vimentin (red), Col I (green), and α-SMA (red). 3D stereo images were obtained from LSCM 3D scanning. (a) Images of lens capsule 3D projections show the holistic views of the subcapsular plaques. Scale bar = 40 μm. (b) Images of lens capsule 3D projections present the depth where the base of the subcapsular plaques could reach from 90-degree rotation projection angle. Scale bar = 40 μm.

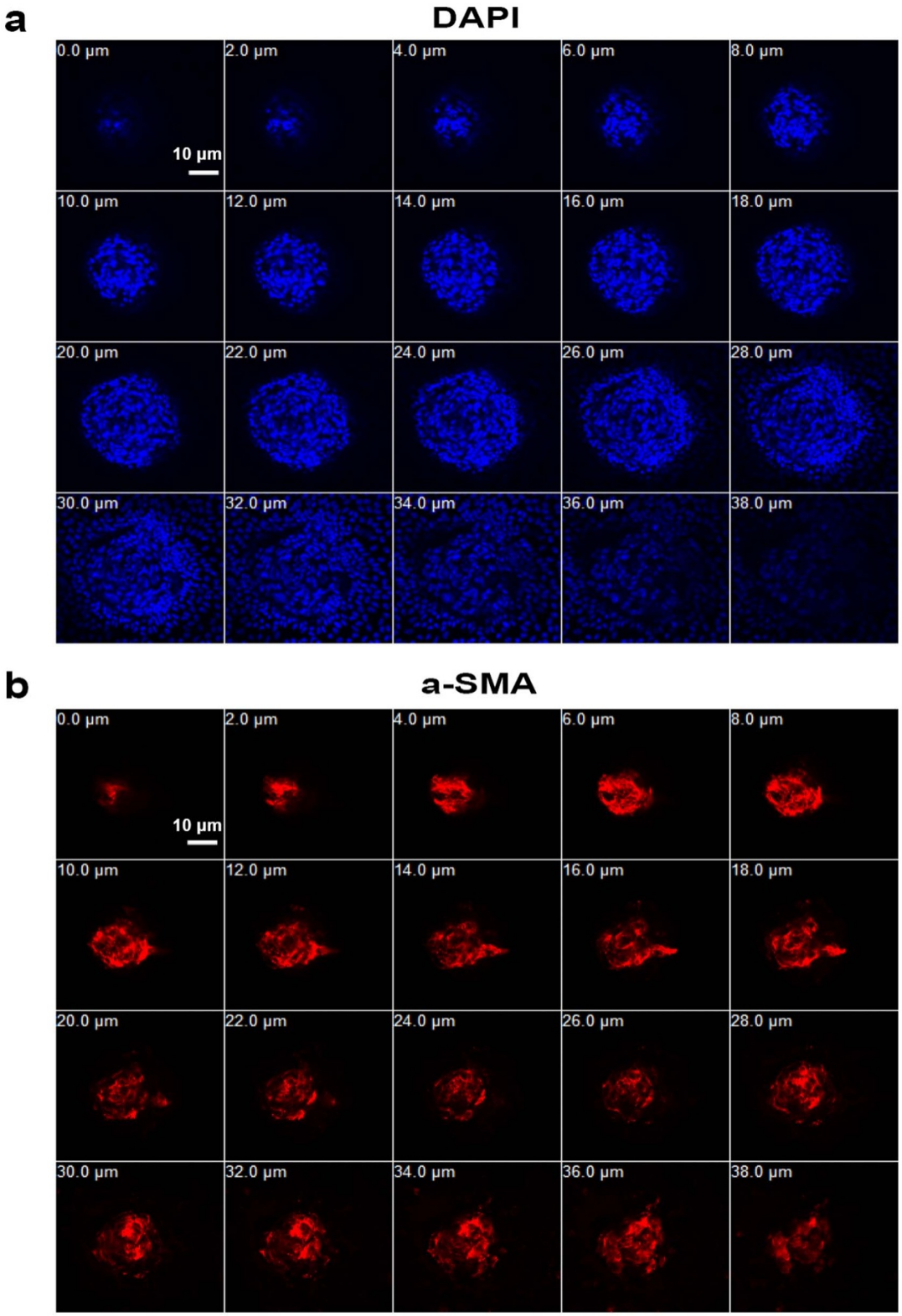

Figure 5 | Continuous, different depth images of lens anterior subcapsular plaque. A series of sectional images of lens anterior capsule whole-mount were acquired from LSCM 3D scanning through setting scanning interval. (a) Serial images of lens anterior capsule whole-mount stained for LECs nuclei with DAPI (blue) show extensive multilayer of cells forming plaque beneath the anterior lens capsule. Scale bar = 10 μm. (b) Serial images of α-SMA distribution (red), the hallmark of the myofibroblasts, in the subcapsular plaque of the injured lens. Scale bar = 10 μm.

injury-induced mouse ASC was accessed using this method. As illustrated in Fig. 7, in the TSA treatment group, the volumes of the subcapsular plaques and the expression of EMT markers α-SMA, Col I and vimentin in the subcapsular plaques were obviously decreased compared with the PBS treatment group at day 7 (Fig. 7b: *, $P<0.05$ *v.* PBS treatment group). Hence, these data indicated that inhibition of HDACs activity with TSA can suppress injury-induced LECs EMT and ASC formation *in vivo*.

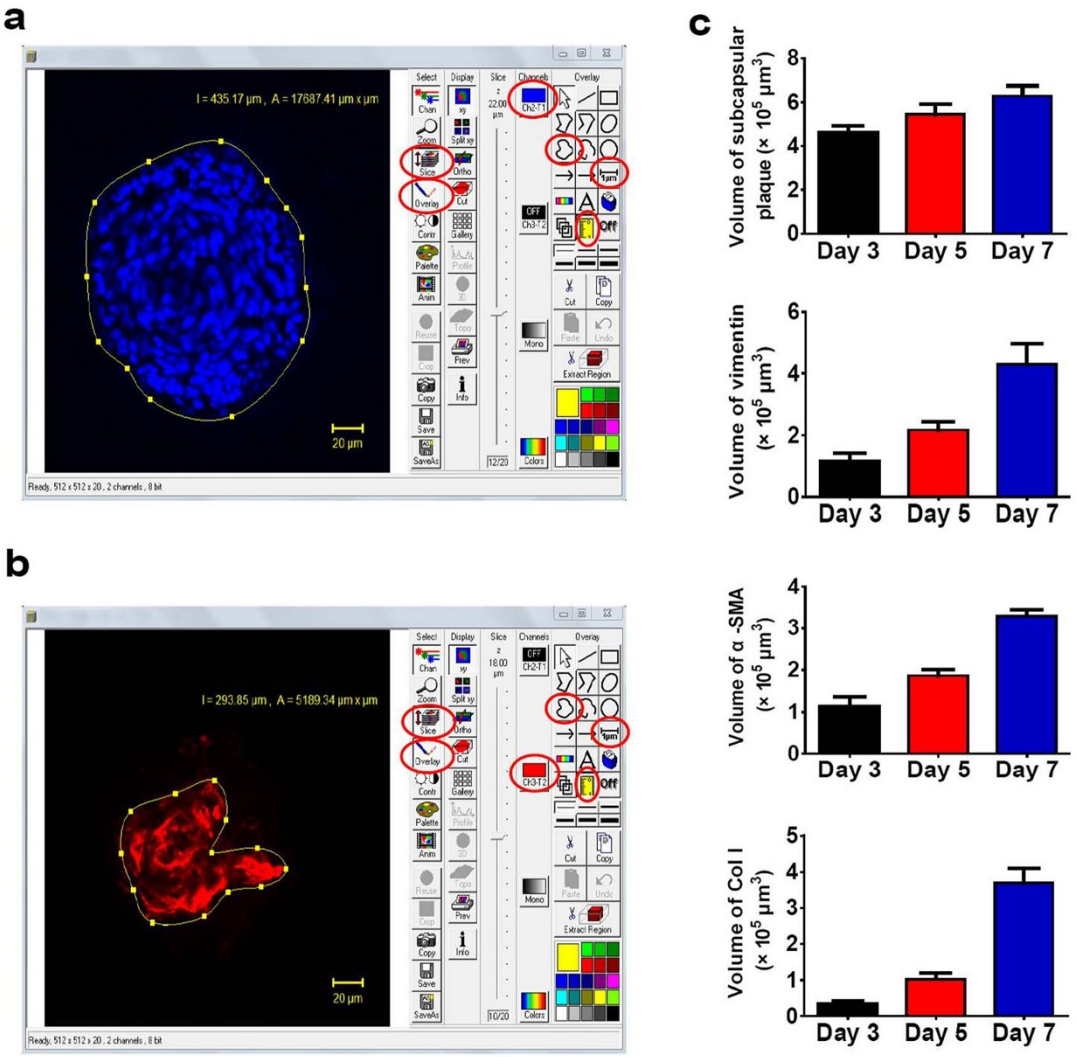

Figure 6 | Quantitative analysis of lens anterior subcapsular plaque volume. (a) Images of lens anterior capsule whole-mount stained for LECs nuclei with DAPI (blue) were acquired from LSCM 3D scanning. Using the LSCM Image Browser software, the subcapsular plaque of lens anterior capsule was manually traced (yellow outline) and the area within the tracing was shown. Screenshot of one representative lens capsule section with the subcapsular plaque area traced. The tools "Slice", "Chan" "Overlay", "Scale bar", "Closed free shape curve drawing" and "Measure" which were used to quantify subcapsular plaque area are highlighted by the red circles. (b) Images of lens anterior capsule whole-mount stained for EMT marker α-SMA (red) were acquired and the area of α-SMA was manually traced (yellow outline). Screenshot of one representative lens capsule section with α-SMA area traced. The tools used to quantify α-SMA area are also highlighted by the red circles. (c) Quantification of the subcapsular plaques volumes and EMT markers distribution at day 3, 5 and 7 according to the formula of the volume of pyramid, and data were expressed as mean ± standard error of the mean (SEM) (n = 6 eyes/group).

Discussion

The mouse lens capsular injury model is a routinely used and well established way for studying LECs proliferation, EMT, ECM compoments deposition and subcapsular plaque formation, as typically seen in ASC and PCO. Since it is easy to handle and it has a relatively short time for the formation of ASC, this model is widely used in a lot of mechanistic studies and therapeutic drug testing. In this study, for the first time, we delineated a simple, good reproducibility and effective method which combines lens capsule whole-mount immunofluorescent staining with 3D confocal morphometric analysis to visualize the spatial features of the subcapsular plaques subtly and quantify the volumes of the subcapsular plaques and EMT markers efficiently and successfully.

LSCM is a type of high-resolution fluorescence microscopy that overcomes the limitations of conventional wide field microscopy[26,27]. It has been widely used for observation of tissue microstructure through 2D fluorescence imaging, however, it also can section relatively thick tissue in different depth along viewing direction, which can be generated as high-resolution 3D images[27]. Laser confocal 3D scanning not only enables researchers to examine the spatial features of tissues, but also provides an approach to observe morphology in detail from any viewing direction and position. More importantly, by using the LSCM Image Browser software in combination, 3D scanning gives us a chance to conduct quantitative analysis. Therefore, LSCM imaging has became a popular research tool which is capable of providing with quantitative data and exquisite stereo images.

Immunofluorescence stained lens capsule whole-mount combined with 3D confocal imaging used in this study has some distinct advantages over conventional histopathologic analysis for monitoring the development of subcapsular plaques. These advantages are as follows: (1) quantitative analysis: It allows continuous sectional scanning and relatively precise quantification of the subcapsular plaque formation *in vivo*. The lens capsule can be serialy scanned from the

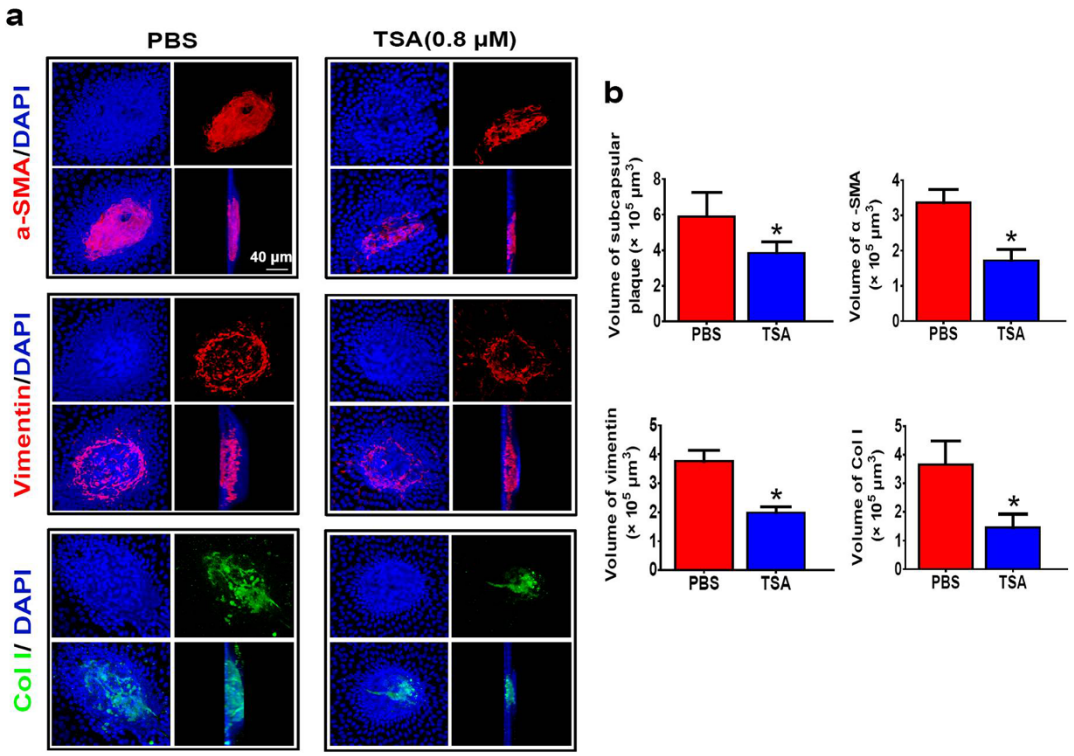

Figure 7 | The HDAC inhibitor TSA suppressed injury-induced ASC in the mouse lens capsular injury model. (a) The anterior capsule of mouse lens is punctured with a needle and 1 μl of 1 μM of TSA was injected into the anterior chamber of the eye immediately after injury with a microsyringe. After 7 days, lens anterior capsules were stained with LECs nuclei (blue) and EMT markers vimentin (red), Col I (green), and α-SMA (red). Images of lens capsule whole-mounts were obtained from LSCM 3D scanning. Scale bar = 40 μm. (b) Quantification of the subcapsular plaques volumes and EMT markers distribution, and data were expressed as mean ± standard error of the mean (SEM) (n = 6 eyes/group).

buttom to the top of the subcapsular plaque, using the LSCM Image Browser software we can readily quantify the volume of the subcapsular plaque *in situ*. (2) 3D reconstruction and display: A series of sectional confocal images containing the whole anterior subcapsular plaque can be reconstructed to 3D stereo images using LSCM Image Browser software. Moreover, these 3D stereo images can also be viewed at any angle and depth, which enables us to obtain detailed information about the spatial features of lens anterior subcapsular plaques. (3) simple procedure: Conventional paraffin section combinged with histological staining quantitative method which requires all the sections from the beginning to the end of the subcapsular plaque to be collected, stained and photographed successfully. That is undoubtedly a technically immense challenge and tedious work. On the contrary, lens capsule whole-mount immunofluorescence staining combined with 3D confocal imaging method is a really simple, time-saving procedure. Lens capsules do not need to be sectioned so that they can be stained as a whole. (4) high throughput, fast, and easy to use: The whole procedure for lens capsule whole-mount immunofluorescence staining lasts less than two days, and commonly used confocal 3D scanning is able to examine one sample in about 15 min. Through setting scanning interval, researchers can obtain a series of continuous, different depth images lightly in one-time. (5) high resolution: We all know that the resolution of confocal scanning is much higher compared with conventional optical microscope and routine fluorescent microscope. Hence, LSCM imaging can provide us with more explicite 2D and stereo images, and detailed information about the spatial features of lens anterior subcapsular plaques.

Of course, lens capsule whole-mount immunofluorescence staining combined with LSCM imaging has its limitations. Compared with conventional histologic analysis, it cannot provide vertical section information of lens anterior subcapsular plaques. In order to observe the vertical section of the subcapsular plaques, we need to combine with conventional histologic analysis, such as paraffin section or cryosection. The other limitation is that it has a higher requirement for the instrument and equipment. LSCM is so expensive that it is not available in many research institutes until now. Clearly, it cannot substitute for conventional histologic analysis.

In conclusion, the new method described herein is a simple, good reproducibility and effective method to visualize the spatial features, and quantify the subcapsular plaques and EMT markers distribution in the mouse lens capsular injury model. By using proliferation markers, it can also be used to examine aberrant cell proliferation in this model. The integration of the mouse lens capsular injury model and this new method provides an opportunity to study the molecular mechanisms of ASC formation as well as the efficacy of new therapies. Moreover, this method may also be applied to other tissues and animal models *in vivo* in the future.

Methods

Mouse lens capsular injury model. All animal studies conformed to the Association for Research in Vision and Ophthalmology Statement for the Use of Animals in Ophthalmic and Vision Research. Animal care and experimental procedures were carried out in accordance with the approved guidelines of Ethics Committee in Animal and Human Experimentation of Sun Yat-sen University. Lens capsular injury in mouse eyes were performed as described previously[14,19]. Briefly, 4 to 6 weeks old C57BL/6J mice were anesthetized generally with intraperitoneal injection of pentobarbital sodium (70 mg/kg) and topically with dicaine eyedrop. After topical application of mydriatic, a small incision was made in the central anterior capsule of the right eye through the cornea with the blade part of a 26-gauge hypodermic needle. The depth of injury was approximately 300 μm or one-fourth of the length of the blade part of the needle, which has been reported previously to lead to the formation of fibrotic tissue around the capsular wound[14,19]. The mice were allowed to heal for 3, 5 and 7 days. At different time points, mice were sacrificed and the eyes were enucleated for the following experiments.

For TSA treatment, 1 μl of 1 μM of TSA was injected into the anterior chamber of the eye after injury with a microsyringe (30-gauge, Hamilton), and the mice were healed for 7 days. Equivalent amount of PBS was injected to all control eyes.

Isolation and fixation of the lens anterior capsule. Injured mice were sacrificed and their eyes were enucleated, and then the eyes were transferred to a culture plate filled with PBS immediately. To isolate the lens anterior capsule, the culture plate containing the eyes was placed under a dissecting microscope, and then the limbus cornea was held with a microforceps and the anterior corneal surface was held with another forceps, after that, the eye globe was split carefully. The cornea, sclera, retina, and iris were removed, leaving the lens merely. The lenses were transferred to 100% methanol immediately and allowed to fix for 1 h at room temperature (RT). After that, the anterior capsules of the lenses were isolated under a dissecting microscope for whole-mount staining, while the posterior capsules were removed and discarded.

Immunofluorescent staining for lens anterior capsule whole-mount. For whole mount lens anterior capsules, the anterior capsules were blocked and permeated with incubation of 1% Triton X-100 in 1% BSA for 1 h at RT. Primary antibodies diluted in PBS were added to immerse the tissues entirely and incubated for 12–24 h at 4°C. On the following day, capsules were washed with PBS containing 0.1% Tween20 (PBST) for 30 min on a rocking board, thereafter, incubated with appropriate secondary antibodies (diluted 1 : 200 with PBS) for 1 h at RT. After washing with PBST for 30 min, capsules were incubated with sufficient volume of DAPI for 10 min to stain the nuclei. Finally, the whole anterior capsule was placed flat on a microscope slide using forceps under a dissecting microscope. The residual PBS on the slide was removed, and the capsule was covered with a coverslip after adding a drop of anti-fade mounting medium. The slides were stored at −20°C in the dark until examination using a fluorescence microscope and a LSCM within a few days.

Primary antibodies against α-SMA, collagen type I (Col I), and vimentin were purchased from Abcam (Cambridge, UK). Alexa Fluor 488-conjugated goat anti-rabbit and Alexa Fluor 555 conjugated donkey anti-mouse secondary antibodies were purchased from Cell Signaling (Danvers, MA).

Immunofluorescent staining for frozen sections. The isolated lenses were embedded in optimal cutting temperature compound and stored at -80°C. Sections (6 μm) were cut using a cryostat, fixed in cold acetone for 15 min, and then incubated with permeablizing solution (0.1% Triton X-100 in PBS) for 5 min. Sections were then blocked with 1% BSA at RT for 1 h followed by overnight incubation with different primary antibodies at 4°C in a humidity chamber. On the next day, the sections were washed with PBST for 15 min on a rocking board, and then incubated with secondary antibodies (1 : 200 dilution) for 1 h at RT. After washing with PBST, sections were incubated with DAPI for 5 min to stain the nuclei. Finally, sections were mounted with anti-fade mounting medium and images were captured using a LSCM.

Obtain 3D images of lens anterior capsule whole-mount. A series of sectional images of each lens anterior capsule whole-mount were acquired from LSCM (LSM510; Carl Zeiss, Overkochen, Germany) or any other equivalent confocal microscope. To generate z-stacks, two-dimensional (2D) images were taken at 2 μm intervals depending on the desirable information of tissue structures. All images were taken by scanning a frame area 512 × 512 or 1024 × 1024 pixels in the x- and y-plane. Generally, it took 10–15 min for a full scanning process from the bottom to the top of the subcapsular plaque, which generated 15–30 optical slices, depending on the scanning interval and the tissue thickness.

Post-recording image processing and analysis. The confocal images containing the whole anterior subcapsular plaque were processed using the Zeiss LSCM Image Browser software (Carl Zeiss, Overkochen, Germany) for 3D stereo projections and analysis. 3D stereo images can be reconstructed using PROJECTION tool and vortically auto played by using ANIM tool or manually viewed at any direction by using SLICE tool. To quantitatively measure the area of the subcapsular plaque in each image, SLICE and OVERLAY tool were used according to the following procedures: Firstly, open target image and then use SLICE tool to view individual image of Z stack one by one by dragging the slider. Secondly, by pressing OVERLAY tool, SCALE, MEASURE and different kinds of DRAWING tool become visible. Draw a scale bar in the image with SCALE button. Thirdly, select an appropriate drawing tool according to the target object, and define the area using the drawing tool and make the necessary adjustment for the area, then click on the MEASURE tool (yellow ruler), the area of the object will be shown on the image. Due to the shape of the subcapsular plaque in this model is similar to trustum of a pyramid, so we calculate the volume of the subcapsular plaque in every two images according to the formula of the volume of pyramid $V_1 = 1/3 \times H \times [S_{up} + S_{down} + \sqrt{(S_{up} \times S_{down})}]$, and the total volume of the subcapsular plaque in one sample equal to the sum total of every two images ($V_{total} = V_1 + V_2 + \ldots\ldots + V_n$). A minimum of 6 capsules were analyzed for each group.

1. McCarty, C. A. & Taylor, H. R. Recent developments in vision research: light damage in cataract. *Invest Ophthalmol Vis Sci* **37**, 1720–1723 (1996).
2. Nathu, Z. *et al.* Temporal changes in MMP mRNA expression in the lens epithelium during anterior subcapsular cataract formation. *Exp Eye Res* **88**, 323–330 (2009).
3. Shin, E. H., Basson, M. A., Robinson, M. L., McAvoy, J. W. & Lovicu, F. J. Sprouty is a negative regulator of transforming growth factor beta-induced epithelial-to-mesenchymal transition and cataract. *Mol Med* **18**, 861–873 (2012).
4. Awasthi, N., Guo, S. & Wagner, B. J. Posterior capsular opacification: a problem reduced but not yet eradicated. *Arch. Ophthalmol.* **127**, 555–562 (2009).
5. Apple, D. J. *et al.* Posterior capsule opacification. *Surv Ophthalmol* **37**, 73–116 (1992).
6. Hodge, W. G. Posterior capsule opacification after cataract surgery. *Ophthalmology* **105**, 943–944 (1998).
7. Srinivasan, Y., Lovicu, F. J. & Overbeek, P. A. Lens-specific expression of transforming growth factor beta1 in transgenic mice causes anterior subcapsular cataracts. *J Clin Invest* **101**, 625–634 (1998).
8. de Iongh, R. U., Wederell, E., Lovicu, F. J. & McAvoy, J. W. Transforming growth factor-beta-induced epithelial-mesenchymal transition in the lens: a model for cataract formation. *Cells Tissues Organs* **179**, 43–55 (2005).
9. Wallentin, N., Wickstrom, K. & Lundberg, C. Effect of cataract surgery on aqueous TGF-beta and lens epithelial cell proliferation. *Invest Ophthalmol Vis Sci* **39**, 1410–1418 (1998).
10. Meacock, W. R., Spalton, D. J. & Stanford, M. R. Role of cytokines in the pathogenesis of posterior capsule opacification. *Br J Ophthalmol* **84**, 332–336 (2000).
11. Eldred, J. A., Dawes, L. J. & Wormstone, I. M. The lens as a model for fibrotic disease. *Philos Trans R Soc Lond B Biol Sci* **366**, 1301–1319 (2011).
12. Allen, J. B., Davidson, M. G., Nasisse, M. P., Fleisher, L. N. & McGahan, M. C. The lens influences aqueous humor levels of transforming growth factor-beta 2. *Graefes Arch Clin Exp Ophthalmol* **236**, 305–311 (1998).
13. Chen, X. *et al.* The epigenetic modifier trichostatin A, a histone deacetylase inhibitor, suppresses proliferation and epithelial-mesenchymal transition of lens epithelial cells. *Cell Death Dis* **4**, e884 (2013).
14. Saika, S. *et al.* Smad translocation and growth suppression in lens epithelial cells by endogenous TGFbeta2 during wound repair. *Exp. Eye Res.* **72**, 679–686 (2001).
15. Oharazawa, H., Ibaraki, N., Lin, L. R. & Reddy, V. N. The effects of extracellular matrix on cell attachment, proliferation and migration in a human lens epithelial cell line. *Exp. Eye Res.* **69**, 603–610 (1999).
16. Saika, S. *et al.* Response of lens epithelial cells to injury: role of lumican in epithelial-mesenchymal transition. *Invest Ophthalmol Vis Sci* **44**, 2094–2102 (2003).
17. Martinez, G. & de Iongh, R. U. The lens epithelium in ocular health and disease. *Int J Biochem Cell Biol* **42**, 1945–1963 (2010).
18. Yamamoto, N., Majima, K. & Marunouchi, T. A study of the proliferating activity in lens epithelium and the identification of tissue-type stem cells. *Med Mol Morphol* **41**, 83–91 (2008).
19. Saika, S. *et al.* Smad3 signaling is required for epithelial-mesenchymal transition of lens epithelium after injury. *Am. J. Pathol.* **164**, 651–663 (2004).
20. Tang, J., Yan, H. & Zhuang, S. Histone deacetylases as targets for treatment of multiple diseases. *Clin. Sci. (Lond)* **124**, 651–662 (2013).
21. Rombouts, K. *et al.* Trichostatin A, a histone deacetylase inhibitor, suppresses collagen synthesis and prevents TGF-beta(1)-induced fibrogenesis in skin fibroblasts. *Exp. Cell Res.* **278**, 184–197 (2002).
22. Xiao, W. *et al.* Trichostatin A, a histone deacetylase inhibitor, suppresses proliferation and epithelial-mesenchymal transition in retinal pigment epithelium cells. *J Cell Mol Med* **18**, 646–655 (2014).
23. Duan, H., Heckman, C. A. & Boxer, L. M. Histone deacetylase inhibitors down-regulate bcl-2 expression and induce apoptosis in t(14;18) lymphomas. *Mol Cell Biol* **25**, 1608–1619 (2005).
24. Henderson, C. *et al.* Role of caspases, Bid, and p53 in the apoptotic response triggered by histone deacetylase inhibitors trichostatin-A (TSA) and suberoylanilide hydroxamic acid (SAHA). *J Biol Chem* **278**, 12579–12589 (2003).
25. Van Beneden, K. *et al.* Comparison of trichostatin A and valproic acid treatment regimens in a mouse model of kidney fibrosis. *Toxicol Appl Pharmacol* **271**, 276–284 (2013).
26. Conchello, J. A. & Lichtman, J. W. Optical sectioning microscopy. *Nat Methods* **2**, 920–931 (2005).
27. Paddock, S. W. Principles and practices of laser scanning confocal microscopy. *Mol Biotechnol* **16**, 127–149 (2000).

Acknowledgments

This study was supported by the grant from the Project of International Cooperation and Exchange NSFC (81320108008).

Author contributions

X.W. and C.X. designed experiments, collected and analyzed data, and wrote the manuscript. L.W. and Y.S. collected and analyzed data. W.W. and L.L. collected data. L.Y. contributed to the manuscript, coordinated experiments and oversaw the project. All authors reviewed the manuscript.

Additional information

Competing financial interests: The authors declare no competing financial interests.

How to cite this article: Xiao, W. *et al.* Quantitative analysis of injury-induced anterior subcapsular cataract in the mouse: a model of lens epithelial cells proliferation and epithelial-mesenchymal transition. *Sci. Rep.* 5, 8362; DOI:10.1038/srep08362 (2015).